Water Resources Research: 5, 1969, 321-340

H27

Global dependence in geophysical records (M & Wallis 1969b)

•***Chapter foreword.*** Venturing well beyond "geophysics," this paper investigates the celebrated sunspot data and reports clear evidence of global dependence. This pioneering finding has been confirmed by many authors.

Numbers of decades in straight log-log plots. The significance of straight doubly logarithmic plots is measured by the length of the straight portion. This paper is very careful on this account.

A matter of layout. To better accommodate the illustrations of this paper, many are printed *not after* the first reference to them, but *before.* •

✦ **Abstract.** A variety of geophysical records are examined to determine the dependence on the lag δ of a quantity called the "rescaled bridge range" and denoted by $R(t, \delta)/S(t, \delta)$. Scientists tend to assume that their records are generated by random processes with a finite population variance and that there is no appreciable dependence between two values of the record at very distant points in time. In cases where these assumptions are both correct, the ratio R/S is proportional to $\delta^{0.5}$. However, as first noted in Hurst 1951, the empirical R/S ratio of hydrological and other geophysical records is of the form $F\delta^H$, where F is a prefactor and the exponent satisfies $H \neq 0.5$. This paper examines new and old data: Hurst's original claims are refined showing his values for the prefactor F to be incorrect and forcing us to discard many of his estimates of H. However, Hurst's main conclusion is confirmed. In our interpretation, the inequality $H \neq 1/2$ expresses that the geophysical records exhibit considerable global statistical dependence. ✦

THIS PAPER PRESENTS AND DISCUSSES SOME GLOBAL PROPERTIES of geophysical records. In particular, it tests the validity of an empirical law that Harold Edwin Hurst discovered during his preliminary studies for the future Aswan High Dam (Hurst 1951, 1956, and Hurst et al 1965). We shall show that this law must be amended, tightened and hedged, but its essential claim will be confirmed. Figure 1. Figure 2. •

INTRODUCTION

"Hurst's law" concerns the dependence on the lag δ of the "rescaled bridge range." It claims that $R(t, \delta)/S(t, \delta)$, takes the form $F\delta^H$, where F is a prefactor and the exponent H is a constant typically differing from 0.5. In this expression, $R(t, \delta)$ is the range of variation between the minimum and maximum values as a function of a particular starting time t and the lag δ while $S(t, \delta)$ is the standard deviation over the same t and δ. Details are given below. Figure 3. Figure 4. Figure 5. Figure 6. Figure 7. •

Table I shows that in most cases $H \neq 0.5$. This inequality has striking consequences. Were the records in question generated by a random process such that observations sufficiently far removed in time can be considered independent, then $R(t, \delta)/S(t, \delta)$ should become asymptotically proportional to $\delta^{0.5}$. This means that Hurst's law would "break" for sufficiently large lags. But no such break has ever been observed. According to M & Wallis 1968{H10} and to the last section of this present paper, it follows that, for all practical purposes, geophysical records must be considered to have an "infinite" span of statistical interdependence. Figure 8. Figure 9. •

"Fractional Gaussian noises," discussed in M & Van Ness 1968{H11} and M & Wallis 1969a{H12,13,14}, are a family of random processes specifically designed to satisfy Hurst's law. Comparison of the figures of the present paper with those of M & Wallis 1969a confirm, in our opinion, that geophysical records can be modeled by fractional noises. The techniques of analysis are found in M & Wallis 1969a. The definitions relative to spectra, being standard, will not be repeated. However, the method of construction of the ratio R/S and the notion of "pox diagram" will be described in detail. Figure 10. Figure 11. Figure 12. •

Extreme caution is required when using R/S to analyze records in which strong cycles are present. This circumstance is documented below, in particular in the case of the sunspot numbers. As a result, R/S may not be the most suitable statistic when strong cycles are present. The marginal distribution of the record, on the contrary has little effect on the behavior of R/S. Figure 13. Figure 14. •

The records studied in this paper fall into three categories of subject matter. Figure 15. Figure 16. •

(1) Recent streamflow, rainfall and temperature records. The longest are the records of annual maximum and minimum stage for the River Nile.

(2) Fossil hydrological records such as tree ring indices, the varve thickness, and other records of geological deposits. Their importance in hydrology will be discussed in the last section of this paper.

(3) Miscellaneous records such as sunspot numbers, earthquake frequencies and directions of river meanders.

The figures in this paper reproduce a small fraction of our present files. We withheld many figures that would be repetitive and a few that would require extensive discussion. The remainder of the paper is devoted to a table of rough estimates of the H-coefficient (the basic parameter of Hurst's law) and to a text devoted to three subjects: the graphical devices we call pox diagrams, pitfalls in the statistical estimation of H and the significance of Hurst's findings in geophysics.

R/S AND POX DIAGRAMS

The following definition of the rescaled bridge range for an empirical record is parallel to the definition of the rescaled range for a random process, as given in M & Wallis 1969a{H13}.

Let $X(t)$ be a record containing T readings uniformly spaced in time from $t = 1$ to $t = T$, and let $X_\Sigma(t)$ designate $\sum_{u=1}^{t} X(u)$. Thus, $\delta^{-1} X_\Sigma(\delta)$ is the

FIGURE C27-1. Construction of the sample bridge range $R(t, \delta)$ {P.S. 1999. The figure in the original reproduces Figure 1 of M & Wallis 1969a{H13}. To reprint it here would be redundant hence it was deleted.

average of the first δ readings, and $\delta^{-1}[X_\Sigma(t+\delta) - X_\Sigma(t)]$ is the average of the readings within the subrecord from time $t+1$ to time $t+\delta$.

$S^2(t, \delta)$ is defined as the sample variance of the subrecord from time $t+1$ to time $t+\delta$, namely

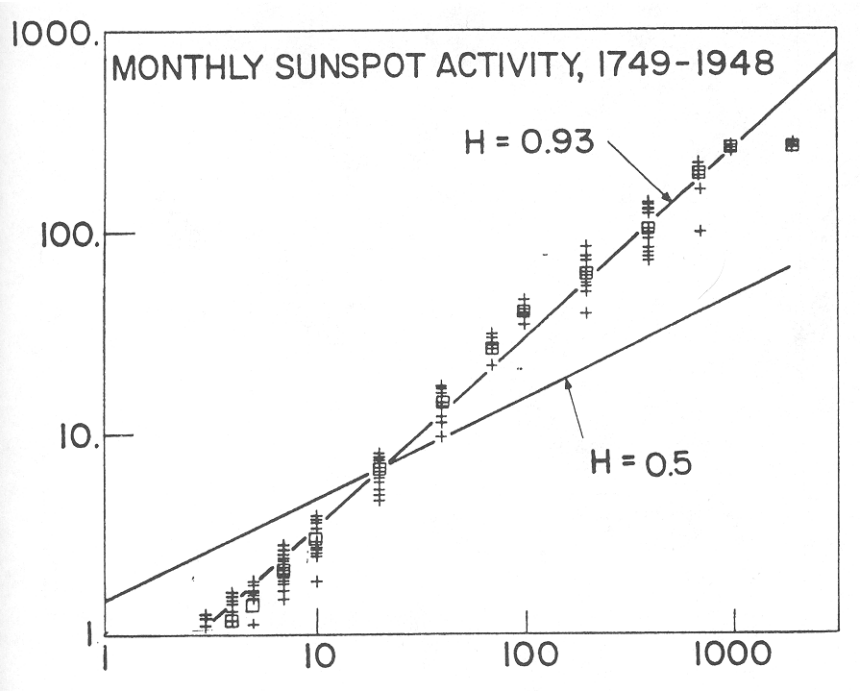

FIGURE C27-2. Pox diagram of logR/S versus logδ for the monthly Wolf numbers of sunspot activity, as reported by Munro 1948 (skewness = 1.04; kurtosis = 3.89.) In the figures of R/S, "time" means "time lag." On this diagram, the slope of the trendline greatly exceeds 0.5. This new observation is much more apparent than the well-known presence in sunspot numbers of a cycle of 11-years = 132 months and perhaps of a cycle of 80 years. Each of these cycles manifests itself mainly by a narrowing of the pox diagram followed by a break shaped like a horizontally laid letter *S*. Before drawing any conclusions from the high apparent value of H for sunspots, the reader should consult M & Wallis 1969c{H25}.

This pox diagram was constructed as follows. The dots (+) correspond to values of the lag δ restricted to the sequence 3, 4, 5, 7, 10, 20, 40, 70, 100, 200, 400, 700, 1000, 2000, 4000, 7000 and 9000. For every δ satisfying $\delta < 500$ we plot 14 dots (+), corresponding to values of t equal to 1, 100, ..., 1400. For every δ satisfying $\delta > 500$, t was made successively equal to 1000, 2000, up to either 8000 or $(T - \delta) + 1$, whichever is smaller.

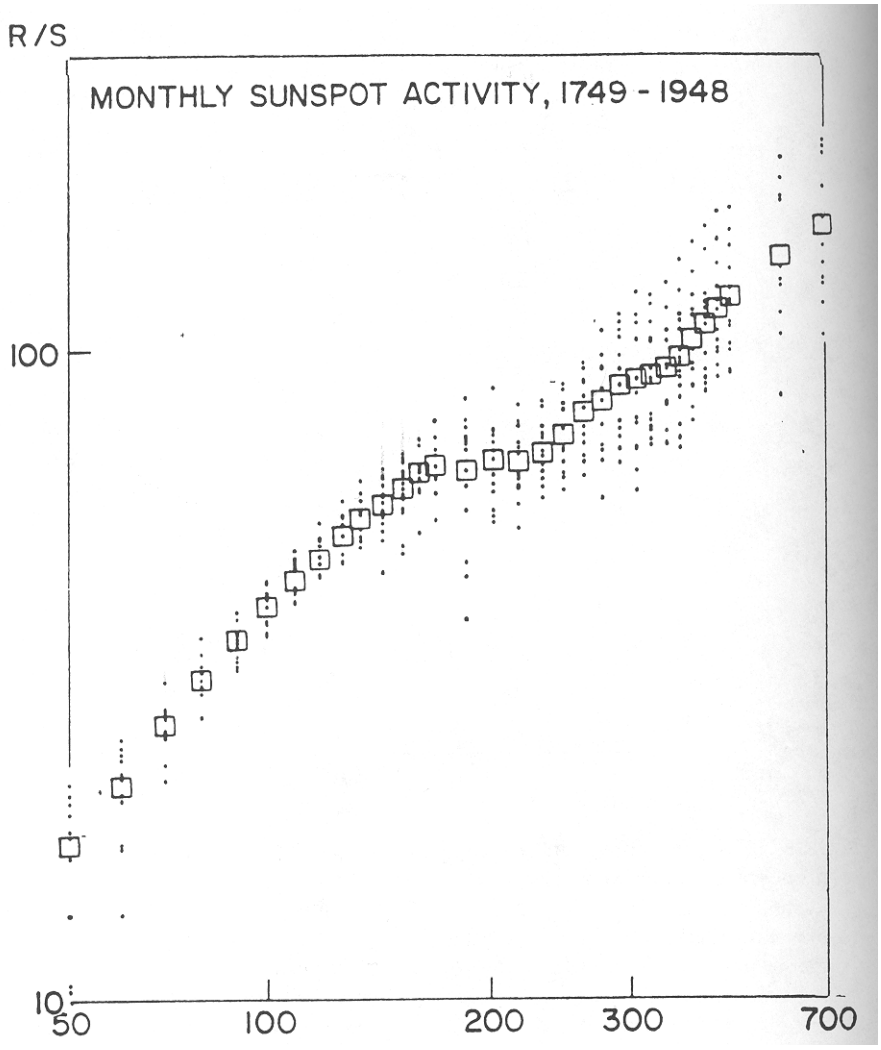

FIGURE C27-3. Detail of a portion of Figure 2. Near the lag corresponding to the 11-year (132 month) cycle, Figure 2 exhibits a "narrowing" followed by a break, which is characteristic of strongly cyclic phenomena. It was imperative to examine this narrowing in detail. In this detailed pox diagram, values of δ are multiples of 10 from 50 to 180, then multiples of 20 from 180 to 500, ending with two additional values at 600 and 700. For each δ, *theselected* values of t were spaced uniformly with increments of 159. Several breaks are clearly visible here.

$$S^2(t, \delta) = \delta^{-1} \sum_{u=t+1}^{t+\delta} X^2(u) - \left[\delta^{-1} \sum_{u=t+1}^{t+\delta} X(u) \right]^2 .$$

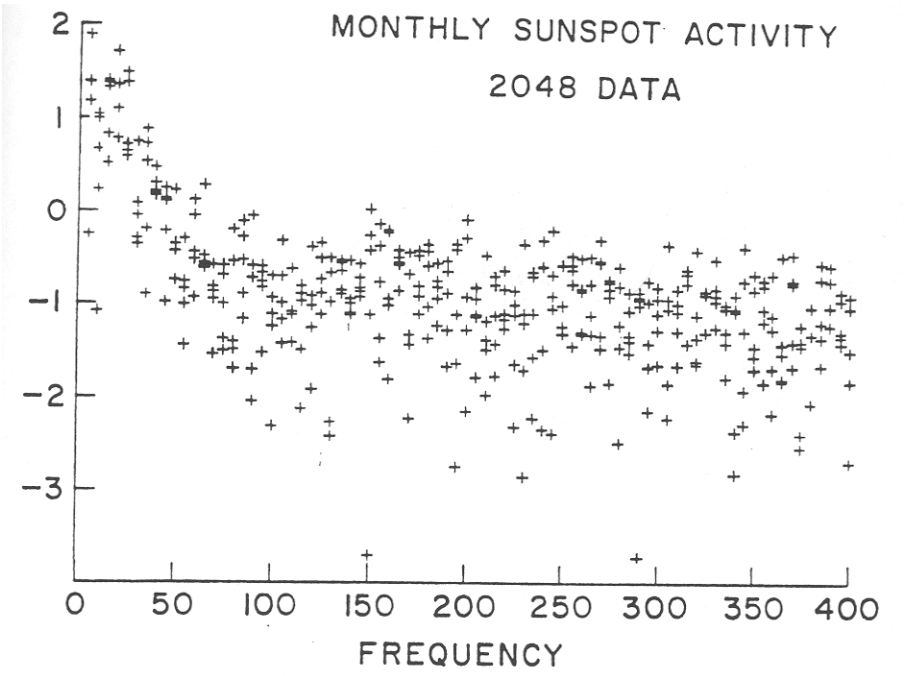

FIGURE C27-4. Pox diagram of the Fourier coefficients of sunspot activity. The total sample was reduced to 2048 data to enable us to use the Fast Fourier Transform computer program. The "frequency" is measured in numbers of cycles per 2048 data. Frequencies are put together in groups of five, each group being of the form $5h$, $5h-1$, $5h-2$, $5h-3$ and $5h-4$, where h takes all positive integer values. The values of the squared Fourier moduli corresponding to frequencies in a group are all plotted above the abscissa corresponding to the highest frequency in such a group, namely $5h$. This procedure introduces a local smoothing that eliminates many apparent cycles and makes it possible to some extent to avoid spectral window processing of the Fourier coefficients (see M & Wallis 1969a, Part 2). Curiously, the well-known 11-year period of the sunspot numbers does not appear as a sharp peak in Fourier coefficients but continues the tendency of the diagram to rise sharply as k decreased. Use of spectral windows on the same data, as in Granger & Hatanaka 1964, p. 66, leads essentially to the same conclusion reached by this pox diagram.

The bridge range $R(t, \delta)$ is illustrated in Figure 1 and is defined as follows:

$$R(t,\delta) = \max_{0 \le u \le \delta} \{X_\Sigma(t+u) - X_\Sigma(t) - (u/\delta)[X_\Sigma(t+\delta) - X_\Sigma(t)]\} - \min_{0 \le u \le \delta} \{X_\Sigma(t+u) - X_\Sigma(t) - (u/\delta)[X_\Sigma(t+\delta) - X_\Sigma(t)]\}.$$

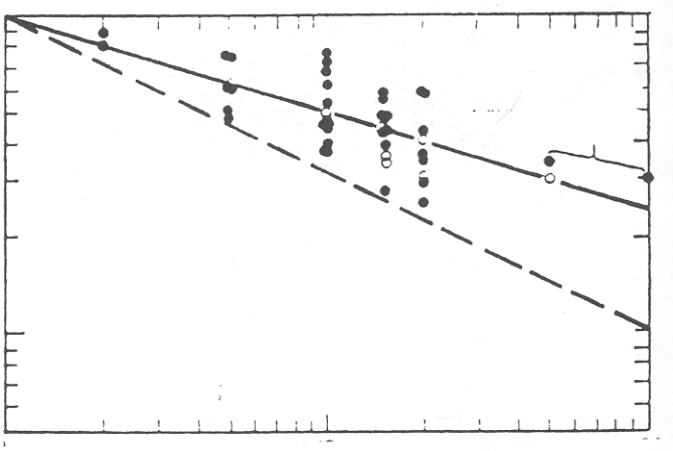

FIGURE C27-5. A superposition of several "variance-time" diagrams. To draw the variance time diagram of a record, one selects a sequence of lags δ (plotted as abscissas). Then, for each δ, one averages δ successive data in a record and one computes the variance of these δ-year averages about the overall average of each sample. The quantity plotted as ordinate is the ratio of this variance for the δ plotted as abscissa, and for $\delta = 1$. Several variance-time diagrams are superposed on the present figure, which does not represent new calculations but is reproduced with the author's permission from Langbein 1956, who used miscellaneous records from Hurst 1956. Superposition has eliminated much of the information in the data, and this figure only shows that every one of the superposed variance-time diagrams is located above the dashed line, which is of slope $H - 0.5$. That line represents the behavior to be expected if observations placed at very distant instants of time had been independent. The fact that the variance decreases less rapidly than expected is a third way of expressing the fact that the R/S pox diagram has a trendline of slope $H > 0.5$ and the fact that the Fourier pox diagram rises steeply for low frequencies. The last two points to the right are for Hurst's data concerning the 1000 year record of Rhoda gauge readings.

The ratio $R(t, \delta)/S(t, \delta)$ is then called a rescaled bridge range. Given the lag δ, the starting t could be given $T - \delta + 1$ different values, but the resulting mass of values of $R(t, \delta)/S(t, \delta)$ is both redundant and unmanageable. The data were replaced by averages but the resulting reduction was, in our opinion, too drastic. The middle ground we chose is to plot the values of $R(t, \delta)/S(t, \delta)$ in the form of what we call a "pox diagram."

To construct a pox diagram, a limited sequence of equally spaced values for the log δ is selected and is marked on the horizontal axis on double logarithmic paper. For each δ, one selects a limited number of starting points t and plots on the vertical axis the corresponding values of $R(t, \delta)/S(t, \delta)$ so obtained. Thus, above every marked value of δ, several points (enlarged into + signs) are aligned. For each δ, the sample average of the quantities $R(t, \delta)/S(t, \delta)$ is indicated by a small square box. The line connecting the boxes weaves through the pox diagram.

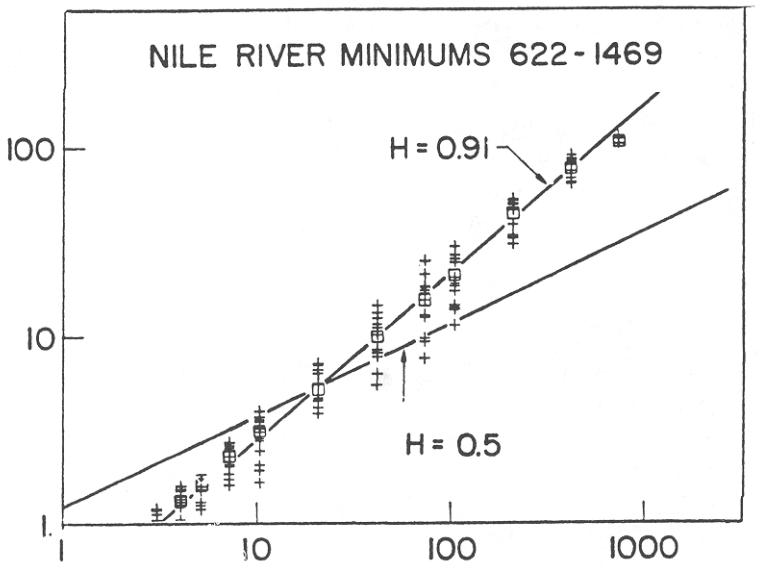

FIGURE C27-6. Pox diagram of logR/S versus log δ for the Nile minimums as reported in Toussoun 1925. (Skewness = 0.32; kurtosis = 3.50.) This pox diagram was constructed as in Figure 2. The Nile is interesting for three reasons: it is the site of the Biblical story of Joseph, which suggested to M & Wallis 1968 the term "Joseph Effect"; it is the river whose flow Hurst's investigations were designed to help regularize; and it is the object of the longest available written hydrological records. The R/S pox diagram of Nile maximums is not plotted because it is extremely similar to the diagram shown in the present figure.

The "trendline" of the pox diagram and Hurst's law. An empirical record is said to satisfy Hurst's law if, except perhaps for very small and very large values of δ, the pox diagram of $R(t, \delta)/S(t, \delta)$ is tightly aligned along a straight trendline, the slope of which will be designated by H. Theory shows that in all cases, $0 < H < 1$. The value $H = 0.5$ has a special significance because it suggests that observations sufficiently distant from each other in time are statistically independent.

M & Wallis 1969b{H25} discusses the concepts of tight alignment along a trendline more precisely and defines several variants (of increasingly demanding scope) of the δ^H law.

Pitfalls in the graphical estimation of *H*

Until better estimation procedures are developed, the exponent H must be estimated graphically from something like the pox diagram. Pitfalls in this approach will now be described.

The "initial transient." For small values of δ, the scatter of the values of $R(t, \delta)/S(t, \delta)$ is large, and various irrelevant influences are felt. Consequently, even if values of R/S for small δ are known, they should be disregarded when drawing conclusions from the pox diagram.

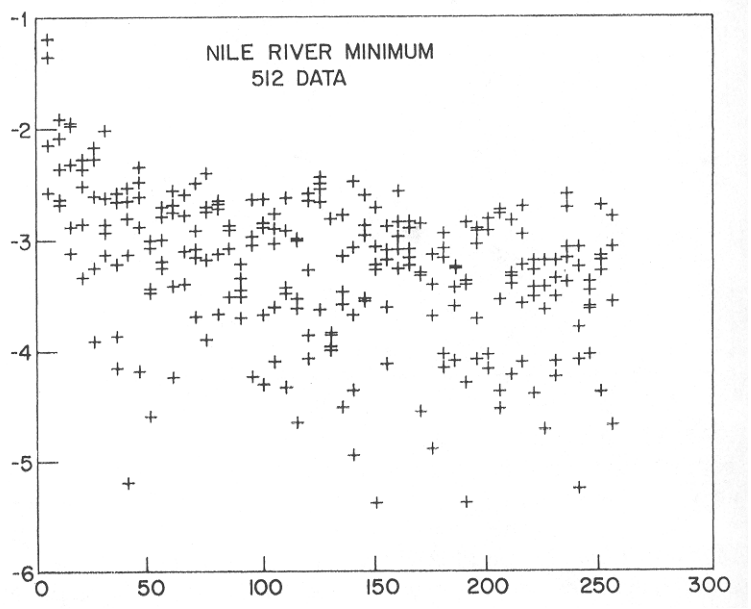

FIGURE C27-7. Spectral pox diagram of Nile minimums. The rise of this diagram, as k decreases, confirms that the value of H is large, as observed in Figure 6.

The "high-lag tightening" of the pox diagram. Let the total sample run from $t = 1$ to $t = T$. For small δ, the starting points t can be selected so that the corresponding sub-samples from $t + 1$ to $t + \delta$ remain nonoverlapping, whereas the number of subsamples remains large. For large δ, the situation is not so ideal. One has the choice between having very few nonoverlapping sub-samples and having a larger number of overlapping sub-samples. Either choice narrows the pox diagram; the former does so because few points are strongly correlated and differ little from each other.

Graphical fitting of a straight trendline. The fact that pox diagrams exhibit an initial transient and a final tightening implies that, when fitting a straight trendline, small and large values of δ should be given less weight than values removed from both $t = 1$ and $\delta = T$.

A warning against an error present in Hurst's initial statement of his law. The statement that we call "Hurst's law" is a significant innovation. Hurst 1951 claimed that the pox diagram of R/S has a trendline going through

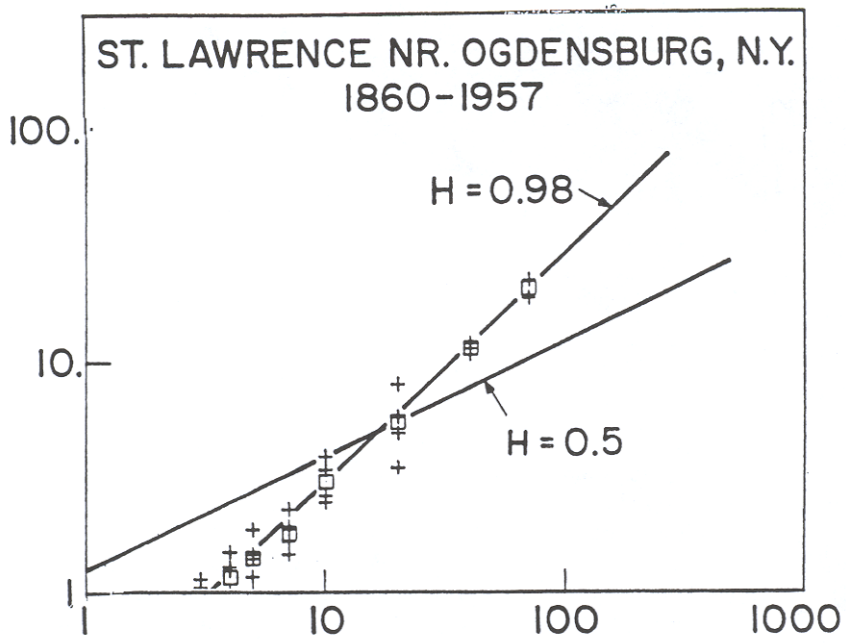

FIGURE C27-8. Pox diagram of logR/S versus log δ for the annual flow of the St. Lawrence River. Data from Professor Yevjevich. (Skewness = - 0.26; kurtosis = 2.7.) This pox diagram was constructed as in Figure 2. It may be observed in Table 1 that the estimate of H would be substantially modified if "carryover" had been taken into account.

the point of the abscissa log2 and the ordinate log1 = 0, which means that Hurst took the prefactor and the exponent to be related by $F = 2^{-H}$. Hurst's claim led to the following estimation procedure. In cases where

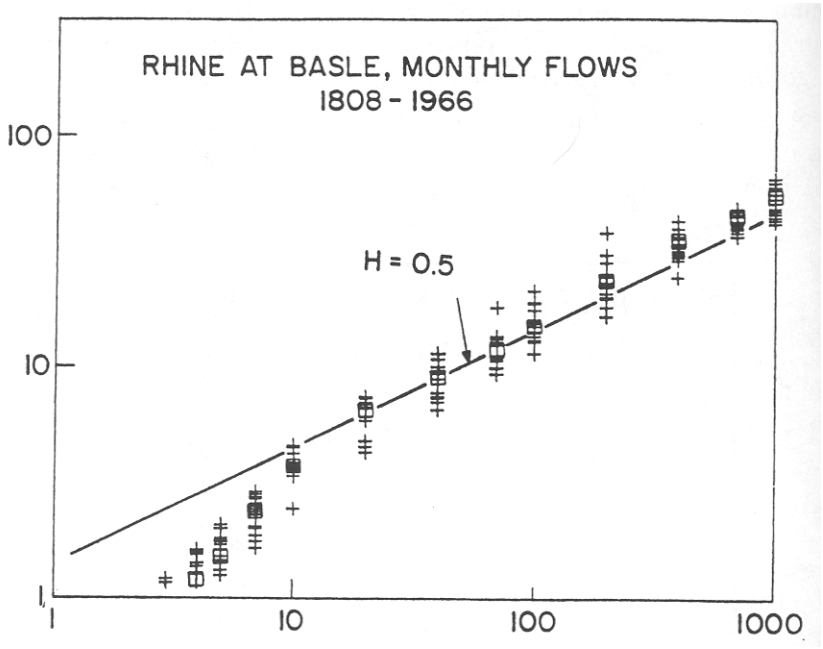

FIGURE C27-9. Pox diagram of logR/S versus logδ for the annual flow of the Rhine River. The data are from de Beauregard 1968. (Skewness = 0.65; kurtosis = 3.01.) This pox diagram was constructed as follows. The logδ was restricted to the values 3, 4, 5, 7, 10, 20, 40, 70, 100, 200, 400, 700, 1000, 2000, 4000, 7000 and 9000. For every δ, we select 15 values of δ, spaced uniformly over the available samples. The Rhine provides a rare example of river flow in which the asymptotic slope of the trendline is very nearly 0.5, meaning that the low-frequency effects that match $H > 0.5$ are absent or weak and that high-frequency effects are not overwhelmed. In our opinion, dealing with the low-frequency effects (when present) takes precedence over dealing with the high-frequency effects to which traditional statistical models are exclusively devoted. In the case of the Rhine, it appears legitimate to use models restricted to high-frequency effects.

$R(t, \delta)/S(t, \delta)$ was known for a single sample from $t+1$ to $t+\delta$, he estimated H to be

$$K(t, \delta) = \frac{\log[R(t, \delta)/S(t, \delta)]}{\log\delta - \log 2}.$$

In cases where $R(t, \delta)/S(t, \delta)$ was known for more than one sample, he averaged the values of the function $K(t, \delta)$ corresponding to all the points of coordinates δ and R/S.

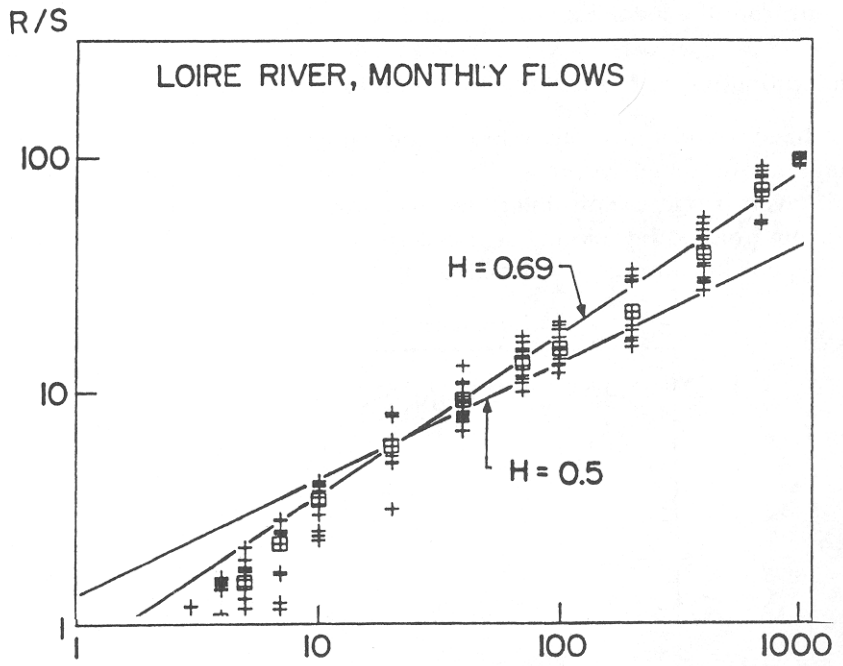

FIGURE C27-10. Pox diagram of $\log R/S$ versus $\log\delta$ constructed as in Figure 9 for the annual flow of the Loire River. The data are from de Beauregard 1968. (Skewness = 1.33; kurtosis = 5.47.) The fact that the value of H is much larger for the Loire than for the Rhine fully confirms the intuitive feeling of French literary geographers for the respective degrees of irregularity of these two rivers. One should, whenever possible, substitute the value of H for the geographer's intuitive descriptions. The latter may, however, be available in cases where the former is unattainable. To make such intuitive knowledge viable, it will be useful to establish a correlation between H and intuition in cases where both are available.

Actual pox diagrams have a straight trendline of slope H that fails to pass through the point of abscissa log 2 and ordinate 0. Hurst's average K is thus a very poor estimate of the slope H. It tends to be too low when $H > 0.72$ and too high when $H < 0.72$. As a result, the trendline and Hurst's method may both suggest identical typical values for H, but Hurst's method greatly underestimated the variability of H around its typical value. The reader may verify the above statements by examining Figures 2 through 7 of M & Wallis 1969a{H12}. For processes such as the stuttering noises of M & Wallis 1969b{H25}, the results obtained using Hurst's method are entirely meaningless. To avoid confusion {P.S. 1999, while honoring Hurst}, we labeled the actual slope with the letter H different from the letter K used by Hurst.

Determination of H for a specific hydrological project

We have found great variability in the values of H measured on R/S pox diagrams of actual records. To explain such variability may prove difficult, even if one is only interested in hydrology. When designing a specific hydrological project, one must, in many cases, be content with an intelligent but imprecise estimated of H. When the data needed to deter-

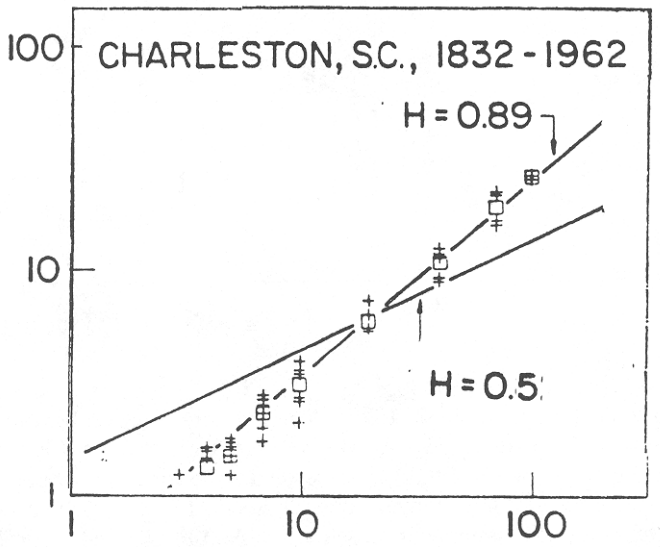

FIGURE C27-11. Pox diagram of logR/S versus logδ for precipitation in Charleston, SC. The data are from the U.S.A. Bureau of the Census 1965. (Skewness = 0.65; kurtosis = 3.5.) Other precipitation records from the same source yield diagrams essentially indistinguishable from this example.

mine H for a certain river are unavailable, related hydrological records may be usable. Regardless of the data used, H is far from 0.5, except for the cases of obviously "well-behaved" rivers such as the Rhine, which is analyzed in Figure 9. However, the difficulty of estimating H is an extremely poor justification for an indiscriminate use of short-memory models that imply that $H = 0.5$.

Warning concerning sunspot records and other data with strong periodic element

To see the effect of strong periodic elements on a pox diagram of R/S, examine Figure 2 relative to the Wolf sunspot numbers. Also examine Figure 3 which is, which enlarges the portion of Figure 2 near a lag of $\delta = 11 = 132$ months, the wavelength of the well-known periodic element in sunspot numbers. One clearly sees (a) a contraction in the scatter of the values of $\log[R(t, \delta)/S(t, \delta)]$ and (b) a break in the trendline, shaped like a horizontally laid reverse S. The partial trendlines before and after the 11-year break have equal slopes, with H greatly exceeding 0.5.

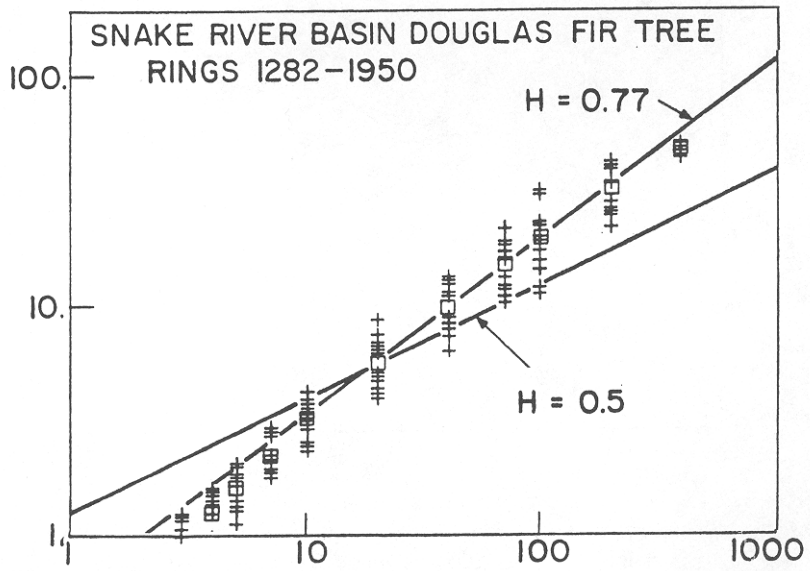

FIGURE C27-12. Pox diagram of $\log R/S$ versus $\log\delta$ for a dendro-chronological series from Schulman 1956. (Skewness = 0.24; kurtosis = 3.60.) Other records in Schulman yield extremely similar pox diagrams. However, the measured values of H vary greatly between different trees in the same general geographical area. This variability confirms that the global characteristics of tree growth are highly sensitive to microclimatic circumstances.

The contraction and the break are both characteristic consequences of the presence of a strong periodic element. In addition, one observes other breaks, corresponding to each subharmonic of $\delta = 11$ years. Since, however, H is very large in the sunspot case, the other breaks are weak. Hence, the presence of a periodic element complicates the picture but does not hide the Hurst phenomenon. Note also that the 80-year cycle reported by Willett 1964, does not show on the spectral box diagram of the sunspot data (see Figure 4), but is detected at the extremity of Figure 2.

In other examples, the basic one year cycle and its subharmonics overwhelm the global interdependence expressed by Hurst's law, and the value of H cannot be inferred graphically from the pox diagram of R/S built with the raw data. The presence of several periodic elements of dif-

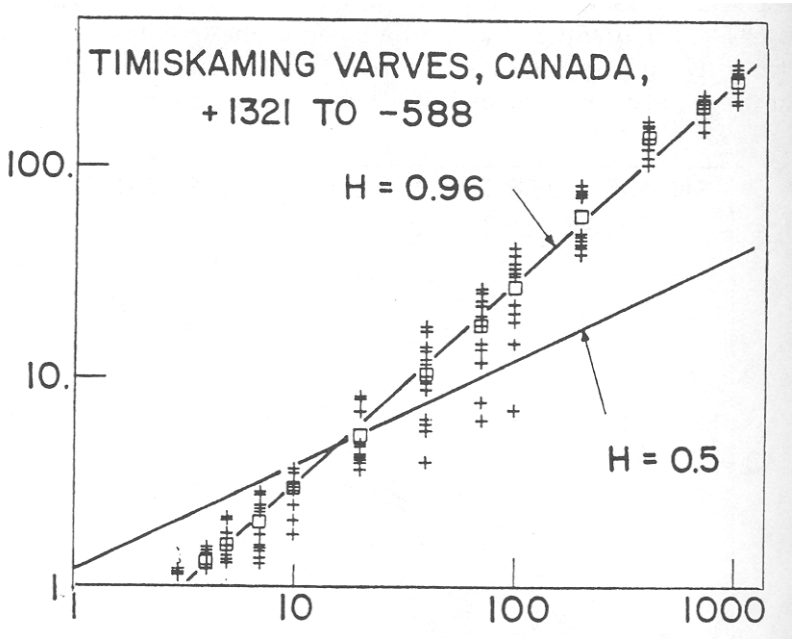

FIGURE C27-13. Pox diagram of logR/S versus logδ for the thickness of the varves in Timiskaming, Canada. The data are from de Geer 1940. (Skewness = 1.03; kurtosis = 6.33.) Other records in de Geer yield extremely similar pox diagrams. The present example was selected because its length is unusual, even among varve records. Every time an unusually long record becomes available, one rushes to check whether or not the slope of the R/S pox diagram breaks back to the value of 0.5 corresponding to asymptotic independence. So far, we are aware of no example of such a break (breaks due to very strong cyclic effects are a different matter).

ferent wavelengths makes the situation even more complicated. For example, add several cyclic components to a fractional noise with a medium-sized value of H. The breaks corresponding to each period and its subharmonics will merge together and yield a pox diagram with a much reduced apparent slope. The slope may fall below 0.5, and the diagram may even appear horizontal. For enormous values of δ, a trendline of slope H will ultimately re-establish itself, but, as we have argued in many other contexts, an asymptotic behavior is of little use either in engineering or in science unless it is very rapidly attained. Examples where strong subharmonics coexist with multiple cycles require lengthy discussion and will not be presented in this paper.

In summary, the pox diagrams of R/S are less useful in the presence of strong periodic elements. Fortunately, most periodic elements in natural records are fairly obvious and can be removed, and the search for "hidden periodicities" is usually fruitless. Below, we shall draw R/S pox diagrams of the corrected records remaining after the periodic elements are removed.

No clear-cut cyclic effect is present in the data analyzed in Figures 5 through 16.

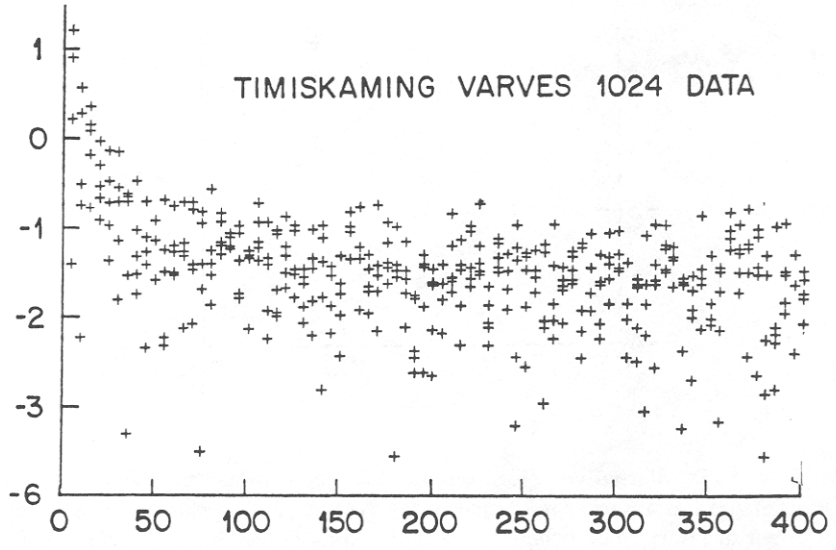

FIGURE C27-14. Fourier pox diagram for Timiskaming varves. Frequencies are plotted on a linear scale of abscissas. The extremely steep low-frequency rise of this diagram confirms the high value of H noted in Figure 13.

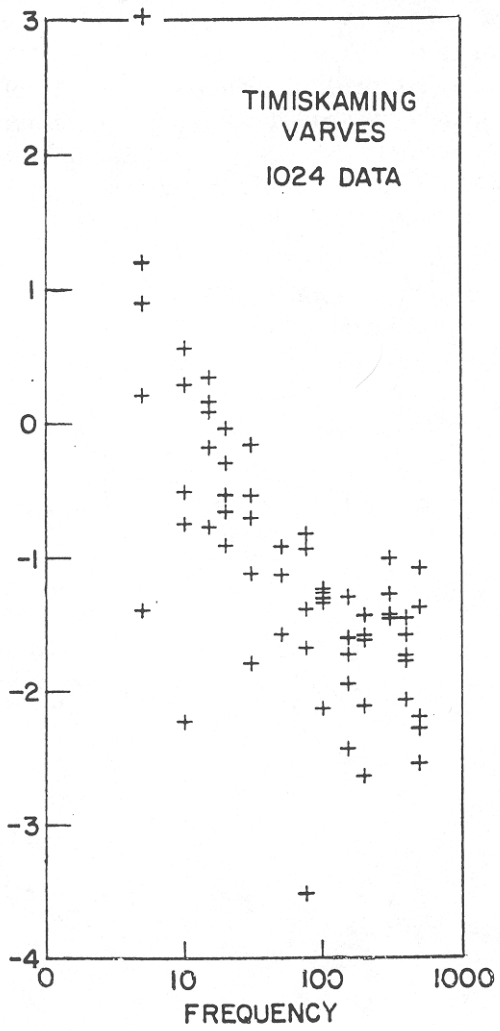

FIGURE C27-15. Alternative plot, on doubly logarithmic coordinates, of the Fourier pox diagram for Timiskaming varves. For clarity, only a small number of Fourier coefficients is plotted. Above the abscissa k, where k is one of the frequencies 5, 10, 20, 30, 50, 75, 100, 150, 200, 300, 400, 500 or 700, we plotted the Fourier coefficients corresponding to the frequencies k, $k-1$, $k-2$, $k-3$ and $k-4$. There is some inconclusive evidence of a dip in spectral density in the neighborhood of frequency 200, hence a wavelength of 5 years.

Significance of Hurst's law in geophysics

Among the classical dicta of the philosophy of science is Descartes' prescription "to divide every difficulty into portions that are easier to tackle than the whole." This advice has been extraordinarily useful in classical physics, because the boundaries between distinct sub-fields of physics are not arbitrary. They are intrinsic, in the sense that phenomena in different fields interfere little with each other and that each field can be studied alone before the description of the mutual interactions is attempted.

Subdivision into fields is also practiced outside classical physics. Consider, for example, atmospheric science. Students of turbulence examine fluctuations with time scales of the order of seconds or minutes, meteorol-

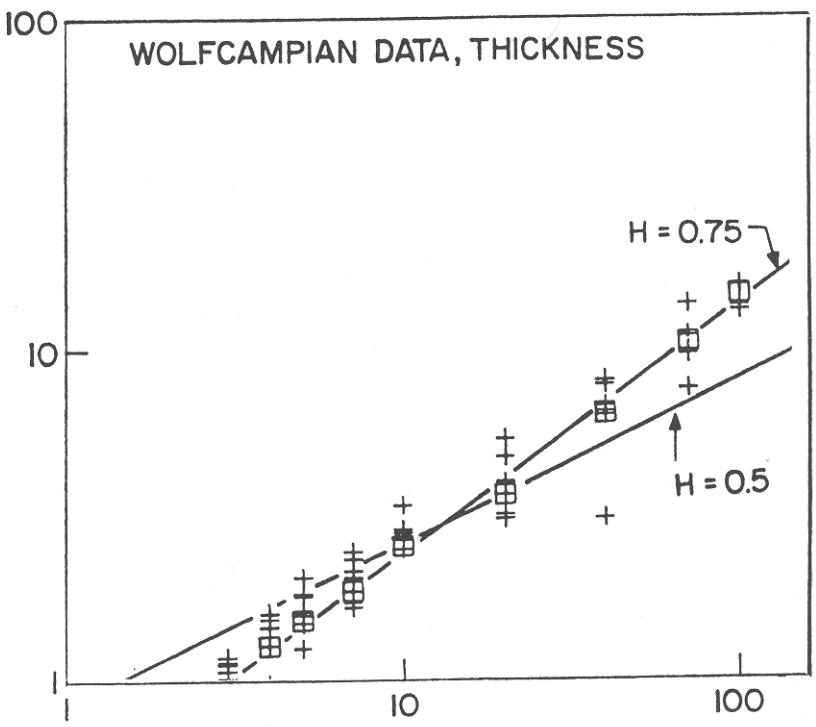

FIGURE C27-16. Pox diagram of $\log R/S$ versus $\log\delta$ for the thicknesses of bedding during the Wolfcampian era in Kansas, which spanned approximately 21 million years. Skewness = 4.60; kurtosis = 32.26; this record is highly nonGaussian) (The data are from G.C. Mann personal communication.) "Time" is measured in cumulated numbers of strata, the n-th items in the record being the thickness of the n-th stratum.

ogists concentrate on days or weeks, specialists whom one might call macrometeorologists concentrate on periods of a few years, climatologists deal with centuries and, finally, paleoclimatologists are left to deal with all longer time scales. The science that supports hydrological engineering falls somewhere between macrometeorology and climatology.

The question then arises whether or not this division of labor is intrinsic to the subject matter. In our opinion, it is not, in the sense that it does not seem possible, when studying a field in the above list, to neglect its interactions with others. We fear, therefore, that the division of the study of fluctuations into distinct fields is mainly a matter of convenient labeling and is hardly more meaningful than either the classification of bits of rock into sand, pebbles, stones and boulders or the classification of enclosed, water-covered areas into puddles, ponds, lakes and seas.

Take the examples of macrometeorology and climatology. They can be defined as the sciences of weather fluctuations on time scales respectively smaller and longer than "one human lifetime." But more formal definitions need not be meaningful. That is, in order to be considered as really distinct, macrometeorology and climatology should be shown by experiment to be ruled by clearly separated processes. In particular, there should exist at least one time span λ, on the order of magnitude of one lifetime, that is both long enough for macrometeorological fluctuations to be averaged out and short enough to avoid climate fluctuations. We shall examine how the existence of such a λ would affect (a) spectral analysis and (b) R/S analysis.

Unfortunately, both spectral and R/S analysis possess limited intuitive appeal. It is therefore useful to first discuss a more intuitive example of the difficulty that is encountered when two fields gradually merge into each other. We shall summarize the discussion in M 1967s of the concept of the length of a seacoast or a riverbank. {P.S. 1999: See also M 1982F{FGN}.} Measure a coast with increasing precision, starting with a very rough length scale and adding increasingly finer detail. For example, walk a pair of dividers along a map and count the number of equal sides of length G of an open polygon whose vertices lie on the coast. When G is very large, the length is obviously underestimated. When G is very small the map is extremely precise, the approximate length $L(G)$ accounts for a wealth of high-frequency details that are surely outside the realm of geography. As G is made very small, $L(G)$ becomes meaninglessly large. Now consider the sequence of approximate lengths that correspond to a sequence of decreasing values of G. It may happen that $L(G)$ increases steadily as G decreases, but it may happen that the zones in which $L(G)$

increases are separated by one or more "shelves" where $L(G)$ is essentially constant. To define clearly the realm of geography, we think it is necessary that a shelf exist for values of G near λ, where features of interest to the geographer satisfy $G \gg \lambda$ and geographically irrelevant wiggles satisfy $G \ll \lambda$. If a shelf exists, one can call $G(\lambda)$ a coast length. A shelf indeed has been observed for many coasts marked by sand dunes and also for many man-regulated coasts (say, the Thames in London). In many cases, however, there is no shelf in the graph of $L(G)$, and the concept of length must be considered entirely arbitrary. Similar comments have been made in other contexts, such as the distinction between the domains of relevance of economics and of the theory of financial speculation see M 1963b{E14}.

After this preliminary, let us return to the distinction between macrometeorology and climatology. It can be shown that, to make these fields distinct, the spectral density of the fluctuations must have a clear-cut "dip" in the region of wavelengths near λ, with large amounts of energy located on both sides. This dip would be the spectral analysis counterpart of the shelf in measurements of coast lengths. But, in fact, no clear-cut dip is ever observed.

Similarly, from the viewpoint of R/S analysis, macrometeorology and climatology are not distinct sciences unless the pox diagram of R/S exhibits distinct macrometeorology and climatology regimes, with an intermediate regime near $\delta = \lambda$ where a variety of configurations is conceivable. To distinguish between macrometeorology and climatology, the intermediate regime of the R/S diagram must be clearly marked and must have a straight trendline of slope 0.5, this region being the R/S analysis counterpart of the shelf in the measurement of coast lengths. The narrower the separating regime, the less clear is the distinction between macrometeorology and climatology. At the limit, our two fields are indistinguishable unless the R/S diagrams are very different for $\delta < \lambda$ and for $\delta > \lambda$. For example, Hurst's law might apply for $\delta < \lambda$ with an exponent $H_1 \neq 0.5$ and for $\delta > \lambda$ with an exponent H_2 differing from both 0.5 and H_1.

When one wishes to determine whether or not such distinct regimes are in fact observed, short hydrological records of 50 or 100 years are of little use. Much longer records are needed; thus, we followed Hurst in searching for very long records among the fossil weather data exemplified by varve thickness and tree ring indices. However, even when the R/S pox diagrams are so extended, they still do not exhibit the kind of breaks that identifies two distinct fields.

We can now return to the claim made on the first page of this paper: the span of statistical interdependence of geophysical data is infinite. By

this we mean only that this span is longer than the longest records so far examined. This gives to the term "infinity" a physical meaning, discussed in M 1963b{E14}, that differs from the definition used in mathematics.

In summary, the distinctions between macrometeorology and climatology or between climatology and paleoclimatology are unquestionably useful in ordinary discourse. But they are not intrinsic to the underlying phenomena and must not influence hydrological design.

One last word concerning explanation. Why is H so well-defined for so many geological data? Why is the Rhine "well-behaved" with $H = 0.5$, while the typical river yields $H > 0.5$? We can state the problem but have no solution to offer. Figure 17.

Description	Apparent H	Moments 3rd	Moments 4th
Nile River Data, Prince Omar Toussoun [1925]			
Annual Maximums 622–1469	0.84	−0.86	7.04
Annual Minimums 622–1469	0.91	0.32	3.50
Data from J. G. Speight (personal communication)			
Moorabool River Meander Azimuths	0.73	0.07	2.82

FIGURE H27-17. Table I values of H and of the 3rd and 4th moments for some geophysical data. (The first and second moments were, in all cases, normalized to be 0 and 1, respectively.) The table continues on the next two pages.

Description	Apparent H	Moments 3rd	Moments 4th
Varve Data from De Geer [1940] Swedish Time Scale			
Haileybury, Canada, +310 to −369	0.80	0.74	4.41
Timiskaming, Canada, +1321 to −588	0.96	1.03	6.33
Sirapsbacken, Sweden, +576 to +257	≈1.00	0.95	3.52
Degeron, Sweden, +499 to 0	0.97	1.10	3.65
Omnas, Sweden, +1399 to +1162	0.65	3.39	23.01
Resele, Sweden, +1399 to +1132	0.67	4.00	26.02
Hammerstrand, Sweden +2000 to +1767	0.85	2.10	9.05
Ragunda, Sweden, +1933 to +1800	0.99	1.59	5.21
Lago Corintos, Argentina, −801 to −1168	0.89	0.85	3.58
Biano, Himalaya Mountains, −1180 to −1279	0.50	1.84	7.82
Sesko, Himalaya Mountains, −1293 to −1374	0.99	0.31	2.20
Enderit River, E. Africa, −406 to −546	0.91	1.07	4.10
Schulman [1956] Tree ring indices			
Table 28, Douglas Fir and Ponderosa Pine, Fraser River, Brit. Col., 1420–1944	0.70	0.19	2.84
Table 30, Douglas Fir, Jasper, Alberta 1537–1948	0.75	0.60	3.34
Table 31, Douglas Fir, Banff, Alberta 1460–1950	0.65	0.32	2.76
Table 33, Douglas Fir and Ponderosa Pine, Middle Columbia River Basin 1650–1942	0.75	0.10	3.20
Table 36, Douglas Fir, Snake River Basin, 1282–1950	0.77	0.24	3.60
Table 38, Limber Pine, Snake River Basin, 1550–1951	0.60	−0.06	3.47
Table 40, Douglas Fir, Upper Missouri River Basin, 1175–1950	≈0.5	0.33	3.14
Table 41, Limber Pine, Upper Missouri River Basin, 978–1950	0.63	0.29	3.71
Table 43, Douglas Fir, North Platte River Basin, 1336–1946	0.70	0.65	3.88
Table 44, Douglas Fir, South Platte River Basin, 1425–1944	0.62	0.21	2.77
Table 45, Douglas Fir, Arkansas River Basin, 1427–1950	0.66	0.03	2.86
Table 49, Mixed species, 3 year means, Colorado River Basin 70 B.C. to 1949 A.D.	0.55	0.25	3.07
Table 50, Douglas Fir, Colorado River Basin, 1450–1950	0.64	−0.15	2.82
Table 52, Pinyon Pine, Colorado River Basin, 1320–1948	0.68	−0.43	3.32
Table 65, Ponderosa Pine, Upper Gila River, 1603–1930	0.69	−0.07	3.25
Table 66, Douglas Fir, Southern Arizona, 1414–1950	0.69	−0.03	3.11
Table 70, Douglas Fir, Upper Rio Grande, 1375–1951	0.65	0.21	2.88
Table 71, Pinyon Pine, Upper Rio Grande, 1356–1951	0.68	−0.23	2.76
Table 72, Douglas Fir, Middle Rio Grande, (Guadalupe), 1650–1941	0.59	0.24	2.87
Table 73, Douglas Fir, Middle Rio Grande, (Big Bend), 1645–1945	0.71	0.59	3.13
Table 75, Ponderosa Pine, S. E. Oregon, 1453–1931	0.58	0.04	3.27
Table 76, Ponderosa Pine, N. E. Calif., 1485–1931	0.78	0.11	3.12
Table 77, Jeffrey Pine, E. Central Calif., 1353–1941	0.72	−0.15	2.93

Description		Apparent H	Moments 3rd	Moments 4th
Table 78, Big-cone Spruce, S. Calif., 1385–1950		0.56	0.11	3.62
Table 79, Ponderosa Pine, S. Calif., 1350–1931		0.72	−0.40	2.89
Table 80, Douglas Fir, W. Central Mexico, 1640–1943		0.86	−0.10	2.40
Table 85, Cipres at Cerro Leon, Argentina, 1572–1949		0.91	0.41	3.41
Data from Statistical History of the United States [1965]				
Annual Precipitation				
Albany, N. Y., 1826–1962		0.87	0.56	3.46
Baltimore, Md., 1817–1962		0.75	−0.06	2.64
Charleston, S. C., 1832–1962		0.89	0.65	3.53
New Haven, Conn., 1873–1962		0.73	0.30	2.33
New York, N. Y., 1826–1962		0.65	0.59	2.89
Philadelphia, Pa., 1820–1962		0.81	0.21	2.85
San Francisco, Calif., 1850–1963		0.64	0.45	3.11
St. Louis, Mo., 1857–1962		0.64	0.63	4.20
St. Paul, Minn., 1837–1962		0.67	0.49	5.15
Data from Ruth B. Simon (personal communication)				
Weekly Derby earthquake frequencies, April 1962–June 1967		0.93	3.99	24.45
Munro [1948] Sunspot data				
Monthly sunspot frequency, 1749–1948		0.96	1.04	3.88
Data from V. M. Yevdjevich [1963], U = Unadjusted for overyear carryover, Y = Adjusted for overyear carryover				
Gota River near Sjotrop-Vanersburg, Sweden, 1807–1957	U	≈0.5	−0.06	2.35
	Y	≈0.5	0.42	2.94
Neumunas River at Smalininkai, Lithuania, U.S.S.R., 1811–1943	U	0.61	0.47	3.15
	Y	0.48	0.61	3.31
Rhine River near Basle, Switzerland, 1807–1957	U	≈0.5	0.14	2.80
	Y	≈0.5	0.23	2.89
Danube River at Orshawa, Romania, 1837–1957	U	≈0.5	0.27	2.26
	Y	≈0.5	0.22	2.53
Mississippi River near St. Louis, 1861–1957	U	0.79	0.29	2.75
	Y	0.68	0.18	2.45
St. Lawrence River near Ogdensburg, N. Y., 1860–1957	U	0.98	−0.26	2.70
	Y	0.69	0.14	2.70
Professor J. C. Mann (personal communication) Data from Paleozoic Era Sediments				
Wolfcampian Section, Kansas	Thickness of beds	0.75	4.60	32.27
	Lithology of beds	0.71	0.25	2.97
Virginian–Desmoinesian Section, Superior, Arizona	Lithology of beds	0.55	0.78	3.27
	Bedding type	0.67	0.19	2.21
Missourian–Atokan Section, Honacker Trail, Utah	Thickness of beds	0.70	3.51	24.81
	Lithology of beds	0.61	−0.05	2.06
	Bedding type	0.58	0.47	2.11
Data from J. de Beauregard [1968]				
Rhine River, Monthly flows, 1808–1966		0.55	0.65	3.01
Loire River, Monthly flows, 1863–1966		0.69	1.53	5.47

&&&&&&&&&&&&& ANNOTATIONS &&&&&&&&&&&&&

Editorial changes. When this paper was reprinted in Barton & LaPointe 1995, new referees suggested small changes, too numerous to be listed, that clarified almost every section. The notation and terminology now match the rest of the book. For example, the function Δ is now called "bridge," $R(t, \delta)$ is now a "bridge range," and "long-run" became "global". The original title was "Some long-run properties of geophysical records".

The R/S analysis of sunspot data showed that phenomena like the Maunder eclipse are very much to be expected. When writing this paper, we were not aware of the "Maunder eclipse." In that period of the 17th century, the Sun was almost spot-free (and Louis XIV, the Sun King, ruled France!) Galileo's discovery of the spots a few decades earlier had suddenly ceased to be confirmed by new observations.

The Maunder eclipse and related slow variations in the number of spots per maximum exemplify the consequences of the very high H (that is, very strong global statistical dependence) reported in this chapter.

Independent role of scaling (that is, scalelessness) in the physics that was emerging in the late 1960s. In classical physics, every field can be subdivided into subfields in intrinsic fashion. My study of the variation of certain speculative prices in M 1963b{E14} suggested that such a subdivision may well be impossible in economics; this paper proves that the same is the case in geophysics. Two comments come to mind.

A) During the late 1960s, analogous developments occurred, absolutely independently, when Leo Kadanoff, Kenneth Wilson, Michael Fisher, and physicists following their lead turned their attention to critical phenomena. By joining the resulting trend in physics, fractal geometry made a contribution to condensed matter physics.

B) Lovejoy 1982 studied the shape of clouds' projections on Earth's surface. When the logarithm of a cloud's perimeter is plotted against the logarithm of its area, one finds the straight line illustrated on page 115 of *FGN*, second and later printings). Clearcut scales supposed to separate the studies of the diverse aspects of weather, but none is visible on this plot.